Ain Shams Engineering Journal (2015) **xxx**, xxx–xxx

Ain Shams University

**Ain Shams Engineering Journal**

www.elsevier.com/locate/asej
www.sciencedirect.com

ELECTRICAL ENGINEERING

# A novel approach for system change pathway analysis using consolidity charts

**Walaa Ibrahim Gabr** *

*Department of Electrical Engineering, Benha Engineering Faculty, Benha University, Egypt*

Received 18 December 2014; revised 16 February 2015; accepted 4 March 2015

**KEYWORDS**

Natural sciences and engineering;
Intelligent systems;
Consolidity charts;
Time driven-event driven-parameters change paradigm;
System change pathway

**Abstract** This paper is directed toward presenting a novel approach based on "***consolidity charts***" for the analysis of natural and man-made systems during their change pathway or course of life. The ***physical significance*** of the consolidity chart (region) is that it marks the boundary of all system interactive behavior resulting from all exhaustive ***internal*** and ***external*** influences. For instance, at a specific event state, the corresponding consolidity region describes all the plausible points of normalized input–output (*fuzzy* or *non-fuzzy*) interactions. These charts are developed as each event step for zone scaling of system parameters changes due to affected events or varying environments "***on and above***" their normal operation or set points and following the "***time driven-event driven-parameters change***" paradigm. Examples of the consolidity trajectory movement in the regions or patterns centers in the proposed charts of various consolidity classes are developed showing situations of change pathways from the unconsolidated form to the consolidated ones and vice versa. It is shown that the regions comparisons are based on type of consolidity region geometric shapes properties. Moreover, it is illustrated that the centerlines connecting consolidity regions during the change pathway could follow some certain type of trajectories designated as "***consolidity pathway trajectory***" that could assume various forms including zigzagging patterns depending on the consecutive affected influences. Implementation procedures are elaborated for the consolidity chart analysis of four real life case studies during their ***conventional*** and ***unconventional*** change pathways, describing: (i) the drug concentration production problem, (ii) the prey–predator population problem, (iii) the spread of infectious disease problem and (iv) the HIV/AIDS Epidemic problem. These solved case studies have lucidly demonstrated the applicability and effectiveness of the suggested consolidity chart approach that could open the door for a comprehensive analysis of system change pathway of many other real life applications. Examples of the fields of these applications are

* Tel.: +20 2 22589764, mobile: +20 1099998762; fax: +20 2 33368748.
E-mail addresses: walaa_gabr@yahoo.com, walaa_gabr@bhit.bu.edu.eg.

Peer review under responsibility of Ain Shams University.

ELSEVIER Production and hosting by Elsevier

http://dx.doi.org/10.1016/j.asej.2015.03.004
2090-4479 

engineering, materials sciences, biology, medicine, geology, life sciences, ecology, environmental sciences and other important disciplines.



## 1. Introduction

The problem of modeling and analysis of system change pathways or their life cycles (course of life) has attracted the interest of many researchers [1–3]. This problem has also been shared by many disciplines as it affects the lifetime of the system. For instance, in engineering and materials the study of this problem is of prime importance as it related to how these systems withstand *internal* and *external* effects such as corrosion, rusts, fatigue, and creep [4–7]. For other disciplines such as medicine and biology, the subject is also very important as it affects the life progress and aging of humans and all living beings [8,9]. In life sciences, ecology and environmental sciences, the problem of system change pathways is still of high priority in solving problems such as river and shores sedimentation and erosion, as well as investigating ecological and environmental growth and balance [10–13].

The study of system change pathways is mainly related to the investigation of all factors affecting such changes. The important parts of these factors are the ones that are taking place "***on and above***" the normal system situation or stands which usually take place outside system control [1–3]. Examples of these affect external or internal excessive influences and happenings affecting the system such as accidents, collisions, impacts, breaks, shocks, collapses, eruptions, and destructions [14,15]. There are no intended timings for such influences and the system is apt to change under their occurrences, which is designated in the literature by "***event-driven***" effect which is governed by the event step "$\mu$" [2]. This is in addition to the well-known "***time-driven***" effect controlled by the physical equations of the system governed by the parameter "$t$".

The relation between the "***time-driven***" versus "***event-driven***" dilemma was the subject of many studies especially by the computer science researchers [16,17]. As the systems handled by computer science are mainly virtually, their developed approaches could not be replicated to physical system due to difference in their nature [18–21]. Such problem was only solved recently by introducing the "***time driven-event driven-parameters change***" paradigm [1–3]. This paradigm states that each event affecting the system "on and above" its normal situation will yield its change of parameters. This is in fact that real life systems are intelligent and store all their affecting events through consecutive changes of parameters. Due to wide changes in the nature and type of systems, such changes will differ from one system to another depending on their internal property denoted by the "***Consolidity Index***" [22–26]. Such index can be calculated from the knowledge of system physical equations.

***Consolidity*** (the act and quality of consolidation) is measured by the system output reactions versus combined input and system parameters reaction when subjected to varying environments and events [1–3]. Moreover, consolidity can govern the ability of systems to withstand changes when subjected to incurring events or varying environments "***on and above***" normal operation during the system change pathway. In fact, consolidity is the scaling factor of managing system changes. It changes all over the lifetime of the system due to its consecutive changes of parameters. Therefore, the in-depth analysis of such index during the system change pathway will definitely lead to much better understanding of such ways, and its future managing and control will help in enhancing such pathways.

In the following section, the methodology of consolidity charts is developed to identify the various regions and patterns of real life systems during their change pathways. Brief backgrounds of some previous subjects will precede such development to help in better understanding of the new development. The paper will then implement this methodology to four different applications to demonstrate the applicability and efficacy of such novel approach for describing their change pathways. These pathway changes are considered for both ***conventional*** and ***unconventional*** systems change pathways behaviors.[1]

## 2. Related work

### 2.1. The "time driven-event driven-parameters change" paradigm

The "***time driven-event driven-parameters change***" paradigm is the central core for investigating the system change pathway or system course of life. This paradigm has three main components as shown in Fig. 1 [1–3]. These components are (i) the lower or time-driven layer, (ii) the upper or event-driven layer, and (iii) the system parameters change mechanism.

The ***first*** component of the lower or time-driven layer is governed by the system physical or dynamical equation(s) of the time state "$t$". Such equations should give an actual form of the system parameters avoiding any virtual, empirical, statistical, or over-simplified forms. These equations are then represent the basic core of any study and are usually can be written in the form of state space representation of the linear, quasi-linear or nonlinear types. A more convenient form of such state space equations is its matrix form, which permits a direct or equivalent investigation of system basic metrics such as ***stability*** and ***controllability***.

The ***second*** component of the upper or event-driven layer is governed by the affecting event or varying environment(s) "***on and above***" system normal situation or stand of the event state $\mu$. Under this event state, the system undergoes various changes corresponding to $\mu = 0, 1, 2, \ldots, m, \ldots, f$, such that $m$ indicates the intermediate state and $f$ designates the end or final state. These events or varying environments are different that ordinary system disturbances that can be usually absorbed by the system with unappreciable effects. One of the important

[1] The term ***conventional*** means linguistically to conform to established practice, accepted standards, or traditional behavior. While the term ***unconventional*** means to act, or exist out of the bounds of standard or standard norms.

Please cite this article in press as: Gabr WI, A novel approach for system change pathway analysis using consolidity charts, Ain Shams Eng J (2015), http://dx.doi.org/10.1016/j.asej.2015.03.004

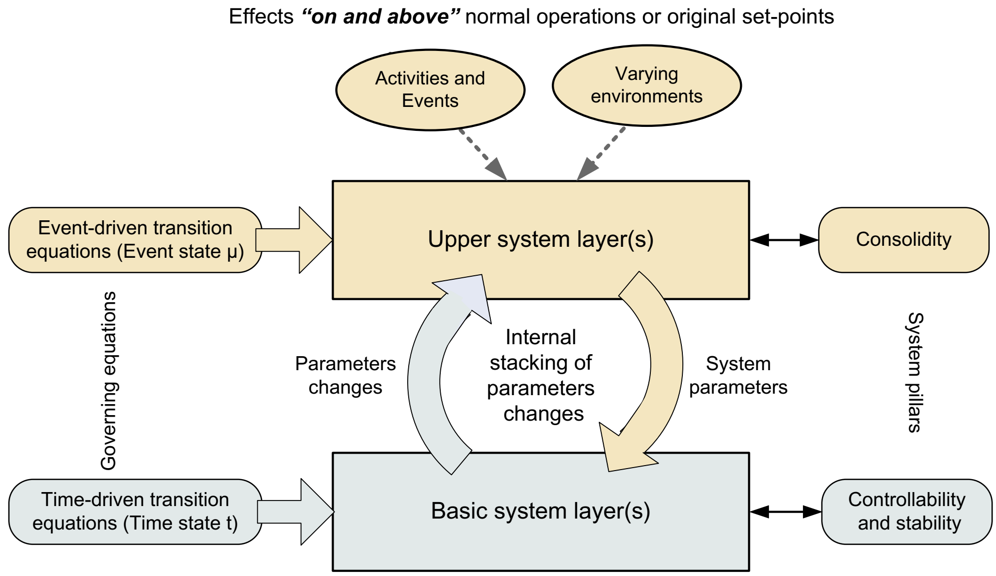


**Figure 1** A schematic diagram depicting the "***time driven-event driven-parameters change***" paradigm [1–3].

system metrics of the upper level is the ***system consolidity*** which is the responsible index for scaling the system parameters changes due to effects as will be defined in the next section. The upper level is activated only with the incoming of each effect or event and yields to the operation of the system parameters change mechanism and the stepping up of the event state such as $\mu \rightarrow \mu + 1$.

The ***third*** component is the parameters change mechanism with each advancement of event or varying environment. A general form of this mechanism can be expressed for any event step $\mu$ as:

$$\text{System parameters}^{(\mu+1)} = \text{System parameters}^{(\mu)} + \Delta\text{System parameters change}^{(\mu)} \text{ and} \tag{1.a}$$

$$\Delta\text{ System parameters change}^{\mu} = \textbf{Function}\ [\text{Consolidity}^{\mu},\ \text{Affected environments or events}^{\mu}] \tag{1.b}$$

such that the term $\Delta$ System parameters change describes the incremental or step parameter change at event clocklike register of state $\mu$. The term "***Affected environments or events***" indicates the overall or effective value, which combines varying environment(s) or event(s) type and strength. The word "**Function**" in (1.b) denotes a general mathematical function or expression. The formal mathematical formulation of the paradigm together with illustrative case studies can be found in [1–3].

It is pointed out that the procedure expressed by (1) follows a *memoryless* or Markovian processes. A ***Markov process*** depends only on the present state and not on how it is arrived in such state. On the other hand, ***non-Markov process*** (memory-based) depends on previous states with lags that change from one system to another. Such type of systems requires obtaining information about the spans of such lags within the system and introduces more terms in the above sequential analysis to represent such lagged components. Straightforward mathematical analysis can then be applied for the extended formulations.

The preliminary investigations of *ad hoc* examples in life sciences, engineering, biology and medicine showed that there are two important forms in real life of **Function** (.) given in (1.b), namely the linear (or linearized) and the exponential relationship for nonlinear cases, given respectively as [2,3,27]:

$$\textbf{Function}\ [\text{Consolidity}^{\mu},\ \text{Affected environments, or events}^{\mu}] = \alpha \cdot \text{Consolidity}^{\mu} \cdot \text{Affected environments or events}^{(\mu)} \tag{2}$$

and

$$\textbf{Function}\ [\text{Consolidity}^{\mu},\ \text{Affected environments, or events}^{\mu)}] = \beta \cdot \exp[\alpha \cdot \text{Consolidity}^{\mu} \cdot \text{Affected environments or events}^{(\mu)}] \tag{3}$$

such that $\alpha$ and $\beta$ are changeability coefficients related to the system physical properties, and "exp" abbreviates exponent [1,2]. In general, Eqs. (1)–(3) and their like's relationships represent the main core of modeling system change in the suggested paradigm.

It can be observed from Fig. 1 that the implementation of the parameters change mechanism is represented as an anti-clockwise process. This representation is made to be in resemblance of all the real life systems of the universe with specific life cycle, where movements anti-clockwise indicate loss of energy and the system stepping toward its progressing states ending by a certain final point or state.

### 2.2. The consolidity methodology

***Consolidity*** is one of the inner properties of system that measure the system susceptibility for withstanding changes. It has also an important role for each system in scaling the affected events or varying environments. The direct way for the calculation of such index is through the use of system physical equations and applies some sort of fuzziness for input and system parameters and calculates the output fuzziness to measure the system overall reaction as described in the followings.

The consolidity methodology for the analysis and design of real-life systems is based on modeling the system input and parameters as fuzzy variables, leading to a corresponding output of the similar fuzzy nature. A system operating at a certain stable original state in fully fuzzy environment is said to be ***consolidated*** if its overall output is suppressed corresponding to their combined input and parameters effect, and vice versa for ***unconsolidated*** systems. ***Neutrally consolidated*** systems correspond to marginal or balanced reaction of output, versus combined input and system.

Let us assume a general system operating in fully fuzzy environment, having the following elements[2]:

***Input parameters***

$$\underline{I} = (V_{I_i}, \ell_{I_i}) \tag{4}$$

such that $V_{I_i},\ i = 1, 2, \ldots, m$ describe the deterministic value of input component $I_i$, and $\ell_{I_i}$ indicates its corresponding fuzzy level.

***System parameters***

$$\underline{S} = (V_{S_j}, \ell_{S_j}) \tag{5}$$

such that $V_{S_j},\ j = 1, 2, \ldots, n$ denote the deterministic value of system parameter $S_j$, and $\ell_{S_j}$ denotes its corresponding fuzzy level.

***Output parameters***

$$\underline{O} = (V_{O_i}, \ell_{O_i}) \tag{6}$$

such that $V_{O_i},\ i = 1, 2, \ldots, k$ designate the deterministic value of output component $O_i$, and $\ell_{O_i}$ designates its corresponding fuzzy level.

We will apply in this investigation, the overall fuzzy levels notion, first for the combined input and system parameters, and second for output parameters. As the relation between combined input and system with output is close to (or of the like type) the multiplicative relations, the multiplication fuzziness property is applied for combining the fuzziness of input and system parameters.

For the combined input and system parameters, we have for the weighted fuzzy level to be denoted as the combined ***Input and System Fuzziness Factor*** $F_{I+S}$, given as:

$$F_{1+S} = \frac{\sum_{i=1}^{m} V_{I_i} \cdot \ell_{I_i}}{\sum_{i=1}^{m} V_{I_i}} + \frac{\sum_{j=1}^{n} V_{S_j} \cdot \ell_{S_j}}{\sum_{j=1}^{n} V_{S_j}} \tag{7}$$

Similarly, for the ***Output Fuzziness Factor*** $F_O$, we have

$$F_O = \frac{\sum_{i=1}^{k} V_{O_i} \cdot \ell_{O_i}}{\sum_{i=1}^{k} V_{O_i}} \tag{8}$$

[2] The ***consolidity concept*** is a general internal property of systems and can be defined using fuzzy sets, rough sets or any other approaches. In this study, fuzzy membership functions are defined through normalized fuzzy levels. It has been previously elaborated that such normalized fuzzy levels concept is identical to that of the conventional fuzzy theory for addition operations and gives average weighted fuzziness interval results of the subtraction operations. Moreover, it yields similar results of multiplication and division operations after ignoring the second order relative variations terms. However, the suggested approach offers additional advantages of linearity, reversibility, simplicity, and applicability [28,29].

Let the positive ratio $|F_O/F_{I+S}|$ defines the ***System Consolidity Index***, to be denoted as $F_{O/(I+S)}$. Based on $F_{O/(I+S)}$ the system consolidity states can then be classified as [22–25]:

(i) ***Consolidated*** if $F_{O/(I+S)} < 1$, to be referred to as "*Class C*".
(ii) ***Neutrally Consolidated*** if $F_{O/(I+S)} \approx 1$, to be denoted by "*Class N*".
(iii) ***Unconsolidated*** if $F_{O/(I+S)} > 1$, to be referred to as "*Class U*".

For cases where the system consolidity indices lie at both consolidated and unconsolidated parts, the system consolidity will be designated as a mixed class or "*Class M*".

Efforts have been made for the compact calculations of the consolidity index with the knowledge of system mathematical formulations [26]. Comprehensive results were attained for handling functions of different dimensionalities, fuzzy analytic geometry, fuzzy vector analysis, functions of fuzzy complex variables, ordinary differentiation of fuzzy functions and partial fraction of fuzzy polynomials. This is in addition to effectively handling of fuzzy matrices covered determinants of fuzzy matrices, the eigenvalues of fuzzy matrices, and solving least-squares fuzzy linear equations. Such derived consolidity index formulations can then be easily embedded within normal mathematics through building special fuzzy functions in as a Matlab Toolbox or inside other like software languages.

In many situations, the direct calculations of the consolidity index could not be straightforward. In such cases, attempts should be made to calculate such system metric through some sort of indirect evaluation. Examples are through calculating the consolidity of system stability measured by eigenvalues, or the controllability of the controllability matrix through its determinant, or through any other representable system metrics.

## 3. Proposed methodology

### *3.1. The consolidity chart*

The concept of implementing the consolidity theory for the analysis and design of control system is of prime importance in investigating the system change pathway. The process commences by plotting for each system its consolidity chart defined as the relation between the ***Output Fuzziness Factor*** $|F_O|$ in the vertical axis ($y$-axis) versus the ***combined System and Parameter Fuzziness Factor*** $|F_{I+S}|$ in the horizontal axis ($x$-axis).

The ***physical significance*** of the consolidity region is that it marks the boundary of all system interactive behavior resulting from all exhaustive ***internal*** and ***external*** influences. For instance, at a specific event state $\mu$, the corresponding consolidity region describes all the plausible points of normalized input–output (*fuzzy* or *non-fuzzy*) interactions of such specific system.

### *3.2. The proposed consolidity pathway*

The implementation of the proposed consolidity charts for investigating the system change pathway undergoes three different stages starting from plotting consolidity points, forming

Please cite this article in press as: Gabr WI, A novel approach for system change pathway analysis using consolidity charts, Ain Shams Eng J (2015), http://dx.doi.org/10.1016/j.asej.2015.03.004

the consolidity regions and ending by drawing the consolidity pathway trajectory as described in the following subsections.

### 3.2.1. First stage – calculation of consolidity points

The first step in forming the consolidity chart is to calculate for each event state $\mu$ a good representable number or collection of consolidity index points. As the system could be affected by wide variety of events or varying environments of different strength, type and direction, some exhaustive selection of such range is to be carried out. This could be based on data gathered on the system during its operation or through some sort of comprehensive surveys of various possible values of effects.

Using (7) and (8), each effect is applied and the results are plotted as a point in the consolidity chart. Each separate point is denoted by the instantaneous consolidity index. All these points are sequentially plotted on the chart. Some redundant points could take place and be also plotted and incorporated in all later calculations. Examples of these points are illustrated in Fig. 2.

### 3.2.2. Second stage – construction of consolidity region

In this stage, the average value of the instantaneous consolidity index points is calculated to obtain the Overall Consolidity index. Such overall index can be represented in the consolidity chart with a straight line with slope equal to the value of the overall index. This line will form the axis of the consolidity zone at the event state $\mu$. The boundary of the region can then be drawn such that all consolidity points are accommodated inside the boundary. Depending on the nature of the problem, such region shape could be of the circular "*C*", elliptical "*E*" or any other geometric type.

The shape and size of each consolidity geometric region determine the feature of system susceptibility to change. For instance, a wider area of the region with big ***Area*** (***A***) means a wide disparity of system reaction to affect influences and vice versa as sketched in Fig. 2. Each shape is described at each event state as follows:

$$R^{(\mu)} = \{R, G, S, C, A, l_1, l_2\}^{(\mu)} \tag{9}$$

such that

| | |
|---|---|
| $\mu$ | event state |
| $R$ | consolidity region symbol |
| $G$ | type of geometry of consolidity region (elliptical "*E*", circular "*C*", etc.) |
| $S$ | slope of overall consolidity index $F_{O/(I+S)}$ |
| $C(x, y)$ | the centroid of the geometric shape $R$ expressed by its horizontal coordinate $x$ (pu) and the vertical coordinate $y$ (pu) |
| $A$ | total area of consolidity region or geometric shape in pu$^2$ where pu abbreviates per unit due to the normalization property of the fuzziness base of the chart |
| $l_1$ | length of major diagonal of the geometric region in direction of overall consolidity index center line (in pu) |
| $l_2$ | length of minor diagonal of geometric region in perpendicular to the overall consolidity index center line (in pu) |
| $l_2/l_1$ | diversity ratio of consolidity points (unitless) |

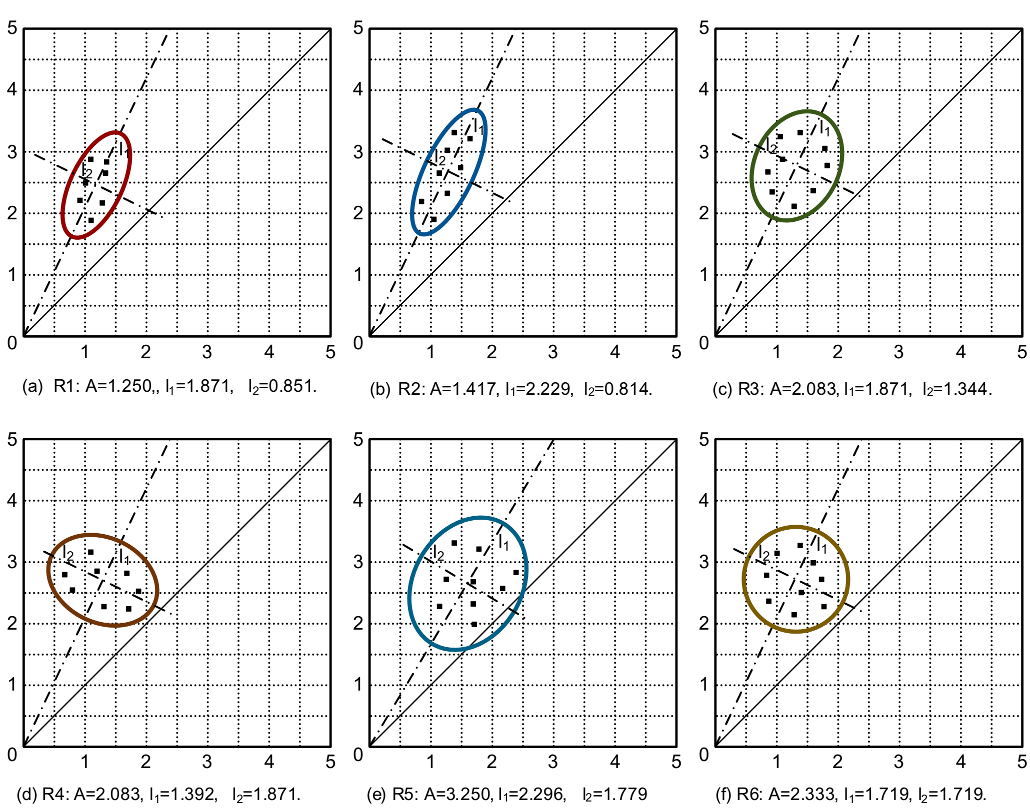


**Figure 2** Examples of different group of elliptical and circular consolidity geometric shapes ($A$: Area, $l_1$: Length of major diagonal and $l_2$: Length of minor diagonals (all dimensions are in pu)).

Please cite this article in press as: Gabr WI, A novel approach for system change pathway analysis using consolidity charts, Ain Shams Eng J (2015), http://dx.doi.org/10.1016/j.asej.2015.03.004

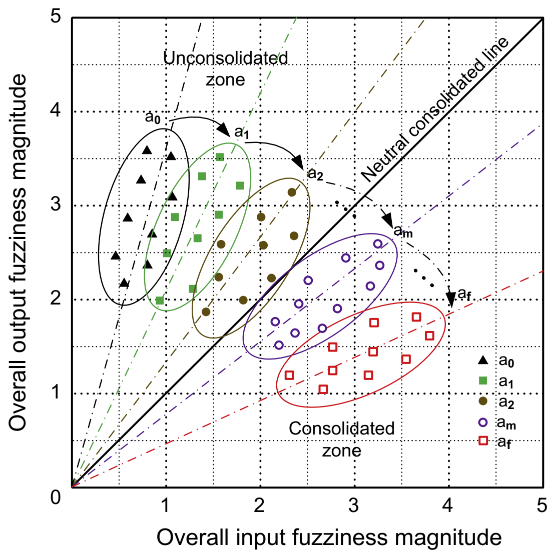

(a) The consolidity chart.

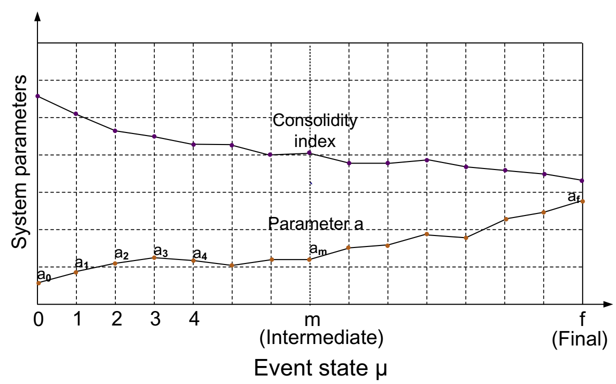

(b) The parameter versus overall consolidity index change per event state.

**Figure 3** Consolidity chart "***Case A***" showing system ***consolidity pathway*** changing from unconsolidated to consolidated state.

For elliptic shapes, the relative lengths of the principal axis provide also information about such susceptibility. A better performance from the consolidity point of view is when the length of $l_1$ (the major diagonal of the region) is much longer than the length of $l_2$ (the minor diagonal of the region). Such characteristics are shown in Fig. 2(a)–(f) having the same overall consolidity index $F_{O/(I+S)}$, with its numerical values are summarized as shown in Table 1.

It follows from Table 1 that shape of Fig. 2(b) is the best from consolidity viewpoint as it has the lowest point diversity shape ratio ($l_2/l_1$). On the other hand, the worst shapes are Fig. 2(d) due to highest points diversity ratio ($l_2/l_1$) and Fig. 2(e) due to its biggest Area $A$ (pu$^2$) with relatively high point diversity ratio ($l_2/l_1$). The circular shape of Fig. 2(f) is of intermediate properties and can be ranked in the middle of this regions group. Each region is then marked with the corresponding event step $\mu$ or with the value of parameter(s) under consideration at such specific event.

### 3.2.3. Third stage – forming of consolidity pathway

In this stage, the process of constructing the consolidity zones is sequentially repeated at each event state $\mu$. This will yield consecutive neighboring consolidity regions, from a starting state, moving to intermediate states, and so on, and then ending with the final state. The combination of these consolidity zones will constitute the changing system consolidity behavior during its change pathway or course of life, and will be referred to as the "***consolidity pathway***". Example cases of such consolidity pathways regions are presented hereafter.

## 3.3. Investigation of representative cases of consolidity pathway

In order to illustrate further the proposed consolidity charts as a comprehensive means for analyzing the system change pathway, three different representable cases are provided as shown in Figs. 3–5. These figures demonstrate three different salient types of such system change pathways as described hereafter.

### 3.3.1. Case A – change pathway from unconsolidated to consolidated state

***Case A*** is shown in Fig. 3(a) and (b) where it is assumed that the change incurring in the system is related to only one specific parameter say "$a$", changing as $a = a_0, a_1, a_2, \ldots, a_m, \ldots, a_f$. Such parameter is considered to be changed after the occurrence of each event state $\mu = 0, 1, 2, 3, \ldots, m, \ldots, f$ such that m indicates an intermediate event state and f designates the final event state.

For this case study change pathway or course of life, it is illustrated by its consolidity chart of Fig. 3(a) that the system undergoes changes shifting its consolidity state gradually step by step with the occurrences of events $\mu$ from the ***unconsolidated*** to ***consolidated*** class at its end state.

### 3.3.2. Case B – change pathway within neutrally consolidated state

***Case B*** is illustrated by Fig. 4(a) and (b) where a governing parameter "$b$" changes with effects during the system change pathway following a zigzag way with a prevailing ascending way to a higher value at its final end state. The case study has moving consolidity zones corresponding to $b = b_0, b_1, b_2, \ldots, b_m, \ldots, b_f$ within the **neutrally consolidated** state. This type

**Table 1** Summary of the shape analysis of consolidity regions shown in Fig. 2.

| Shape no. | Region symbol ($R$) | Shape type ($G$) | Area $A$ (pu$^2$) | Length of major diagonal $l_1$ (pu) | Length of minor diagonal $l_2$ (pu) | Diversity ratio ($l_2/l_1$) | Ranking from consolidity viewpoint |
|---|---|---|---|---|---|---|---|
| a | $R1$ | $E$ | 1.250 | 1.871 | 0.851 | 0.455 | 2 |
| b | $R2$ | $E$ | 1.417 | 2.229 | 0.814 | 0.365 | 1 |
| c | $R3$ | $E$ | 2.083 | 1.871 | 1.392 | 0.744 | 3 |
| d | $R4$ | $E$ | 2.083 | 1.392 | 1.871 | 1.344 | 6 |
| e | $R5$ | $E$ | 3.250 | 2.296 | 1.779 | 0.775 | 4 |
| f | $R6$ | $C$ | 2.333 | 1.719 | 1.719 | 1.000 | 5 |

Please cite this article in press as: Gabr WI, A novel approach for system change pathway analysis using consolidity charts, Ain Shams Eng J (2015), http://dx.doi.org/10.1016/j.asej.2015.03.004

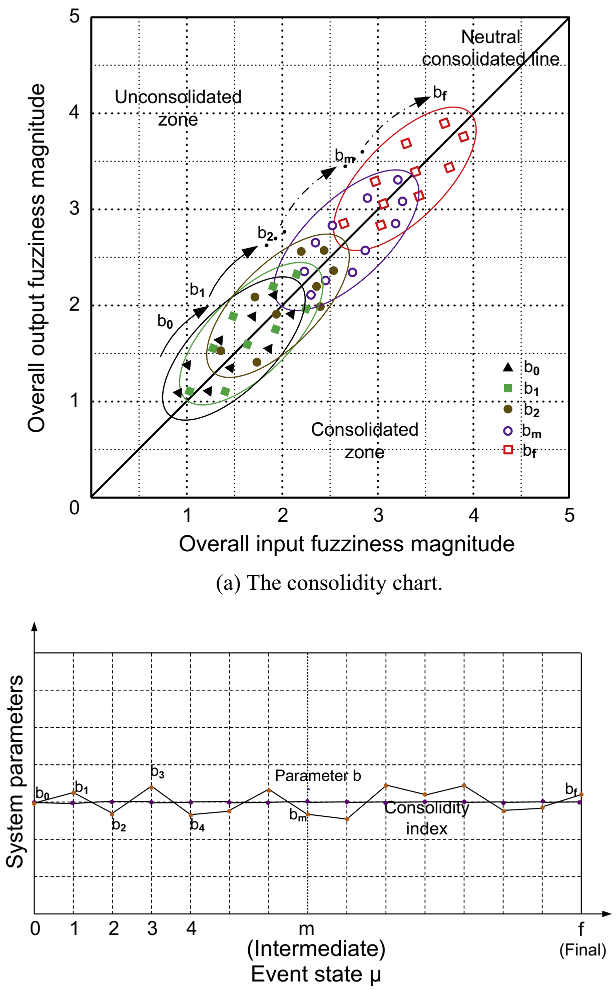


(a) The consolidity chart.

(b) The parameter versus overall consolidity index change per event state.

**Figure 4** Consolidity chart "***Case B***" showing system ***consolidity pathway changing*** within the consolidated class.

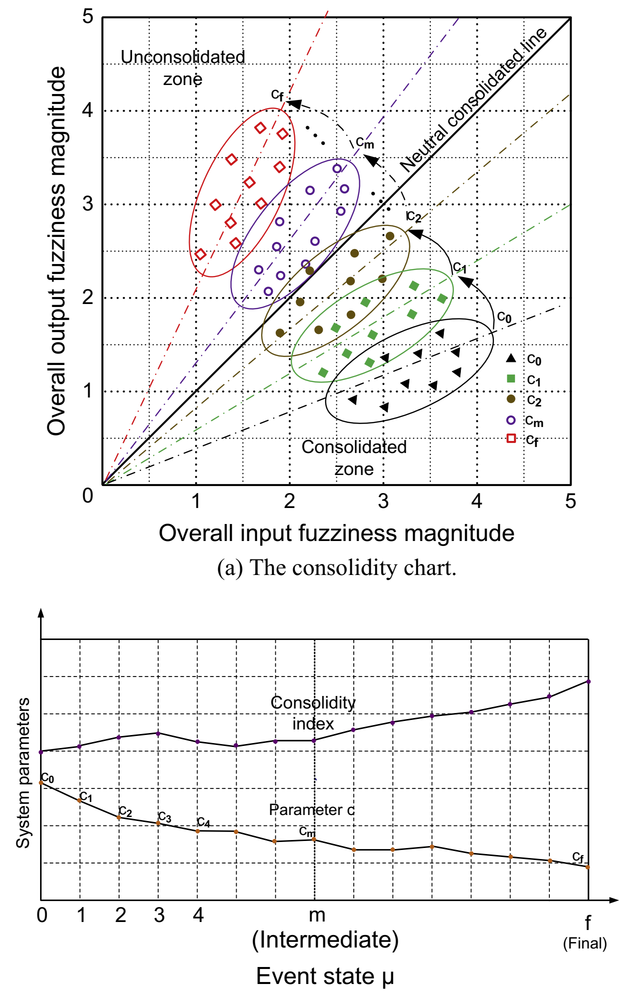


(a) The consolidity chart.

(b) The parameter versus overall consolidity index change per event state.

**Figure 5** Consolidity chart "***Case C***" showing system ***consolidity pathway*** changing from the consolidated to unconsolidated class.

of systems commences as neutrally consolidated and changes slightly but still remains within the same class. The corresponding consolidity index remains within such neutrally consolidated sate.

### *3.3.3. Case C – change pathway from consolidated to unconsolidated state*

***Case C*** is illustrated by Fig. 5(a) and (b) where a governing parameter "$c$" is changing depending on the event state $\mu$ as $c = c_0, c_1, c_2, \ldots, c_m, \ldots, c_f$. This case is opposite to Case A where the consolidity zone moves during change pathway or course of life from consolidated state gradually ending at the unconsolidated state.

In general, the ***consolidity pathway trajectory*** (connecting centerline of consolidity regions) in real life situation follow a certain zigzagging pattern path as shown for the two cases schematized in Fig. 6(a) and (b), illustrating two change pathways from unconsolidated to consolidates state and vice versa. In such situation, the overall consolidity index changes in a ascending (or descending) manner depending on the type and direction of affected influences or effects at each event step $\mu$, but the prevailing value at the end will be an overall increase (or decrease).

In real life applications, it is pointed out that other mixed consolidity chart patterns may take place depending on the variability of the strength, type and direction of the event state. Furthermore, typical ranges of the consolidity indices in the described consolidity charts based on previous real life applications are as follows: very low (<0.5), low (0.5–1.5), moderate (1.5–5), high (5–15), and very high (>15) [2,3]. Each application of consolidity chart of system change pathway should be considered as a ***specific case by case*** problem. Such aspect will be further elaborated when handling the various real life applications given in the following sections.

## 4. Implementation to drug concentration production problem

### *4.1. Model description*

The first case study represents a ***man-made*** system operation during its course of operational life. It is regarding one of the common processes in pharmaceutical industry manufacturing named as drug concentration production. The system in its simplest form is manufactured as two equal (or non-equal compartments) separated by a special membrane where diffusion takes place to obtain the necessary substance concentration [30].

In this case study, let us consider the drug concentrations for two compartments physical system of different volumes separated by a membrane. The drug can flow through such membrane from compartment #1 to #2, and vice versa as shown in Fig. 7. All system parameters are modeled as fuzzy variables.

Let us now introduce the main parameters of the system as follows [10]:

| | |
|---|---|
| $V_i$ | the volume of compartment $i = 1, 2$ |
| $x_i(t)$ | the amount of the drug in compartment $i = 1, 2$ respectively at time $t$ |
| $A$ | the area of membrane between the two compartments |
| $a_{12}$ | proportionality coefficient rate of flow of the drug from #2 to #1 |
| $a_{21}$ | proportionality coefficient rate of flow of the drug from #1 to #2 |
| $a_2$ | proportionality coefficient rate of flow of the drug from #2 to outside |

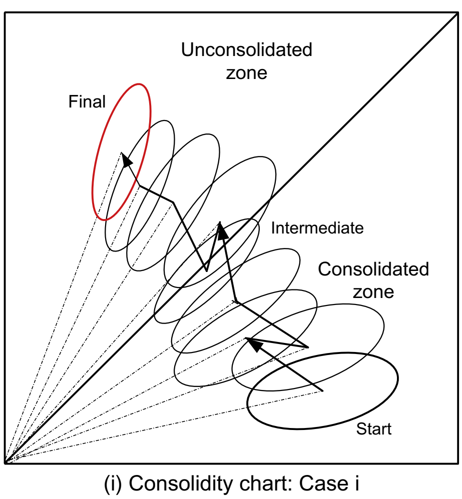


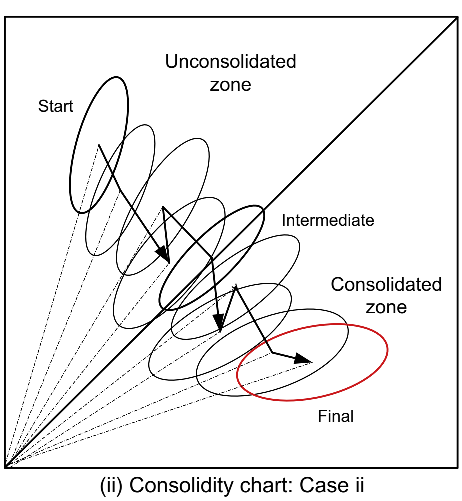


**Figure 6** Two examples of consolidity pathway trajectories having zigzagging patterns during the system course of life.

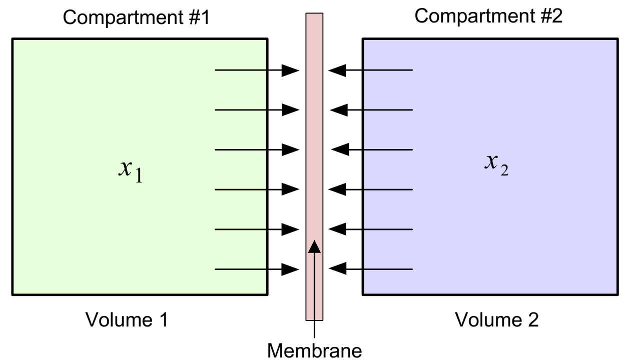


**Figure 7** A diagram describing operation of the drug concentration production problem.

The system model can be expressed by the two linear differential flow equations [10]:

$$\dot{x}_1 = a_{21} \cdot A \cdot (x_2/V_2) - a_{12} \cdot A \cdot (x_1/V_1) \quad (10)$$

and

$$\dot{x}_2 = a_{12} \cdot A \cdot (x_1/V_1) - a_{21} \cdot A \cdot (x_2/V_2) - a_2 \cdot (x_2/V_2) \quad (11)$$

Eqs. (10) and (11) can be simplified by substituting: $b_{12} = a_{12} \cdot A/V_1$, $b_{21} = a_{21} \cdot A/V_2$, and $b_2 = a_2/V_2$. This yields the simplified linear differential equation [11]:

$$\dot{x}_1 = b_{21} \cdot x_2 - b_{12} \cdot x_1 \quad (12)$$

and

$$\dot{x}_2 = b_{12} \cdot x_1 - (b_{21} + b_2) \cdot x_2 \quad (13)$$

The problem can then be expressed in the state space form [10]:

$$\begin{bmatrix} \dot{x}_1 \\ \dot{x}_2 \end{bmatrix} = \begin{bmatrix} -b_{12} & b_{21} \\ b_{12} & -(b_{21} + b_2) \end{bmatrix} \cdot \begin{bmatrix} x_1 \\ x_2 \end{bmatrix} \quad (14)$$

having the corresponding characteristic equation using Laplace Transform as follows:

$$s^2 + s \cdot (b_{12} + b_{21} + b_2) + b_{12} \cdot b_2 = 0 \quad (15)$$

The two roots of (15) indicate the stability of this system, and must lie in the Left Half s-Plane. The system is less stable if the left half s-plane poles move toward the origin [1,2]. The consolidity analysis of this case study will be based on calculating the consolidity of the eigenvalues of the system during the system change pathway.

### *4.2. Consolidity chart for conventional system change pathway behavior*

For the present case study, it can be seen that the parameter $b_2$ that defines the proportionality coefficient rate of flow of the drug from #2 to outside can be affected by the deterioration and aging of consecutive processes. This deterioration could lead to the gradual reduction or chocking of the outside flow from the drug concentration system. To demonstrate such gradual aging and deterioration of the system we will consider a gradual change of such parameter from a certain design value of $b_2^{(0)} = 2.0$ to a final or end value of $b_2^{(f)} = 0.1$. The parameter changes in between gradually depending on the condition adjacent to the drug concentration unit.

For various conventional change pathway values of the parameter $b_2$, the consolidity analysis is carried out for the combined poles of the system and the results are shown in Table 2. The consolidity chart of the problem is sketched in Fig. 8, for seven chosen regions (three at the system beginning of its course of life, two at its intermediate life, and two at its ending life). The figure demonstrates the consolidity pathway trajectory during the change of parameter $b_2$ as moving from a starting point of high consolidity index of $F_{O/(I+S)}$ = 11.2100 (***unconsolidated state***) and is reduced gradually to attain at the end a low consolidity value of $F_{O/(I+S)}$ = 1.0771 (nearly ***neutral consolidated state***).

### *4.3. Consolidity chart for unconventional system change behavior*

Let us now investigate the ***unconventional*** change pathway behavior of the above drug concentration production problem

**Table 2** Consolidity pathway results of the drug concentration production problem.

| Aspect | Input parameters | | Consolidity indices (based on system eigenvalues) | | | | | | |
|---|---|---|---|---|---|---|---|---|---|
| | $b_{12}$ | $b_{21}$ | $b_2^{(0)}$ | $b_2^{(1)}$ | $b_2^{(2)}$ | $b_2^{(m)}$ | $b_2^{(m+1)}$ | $b_2^{(f-1)}$ | $b_2^{(f)}$ |
| Value | 0.3 | 0.5 | 2.0 | 1.8 | 1.6 | 1.0 | 0.8 | 0.2 | 0.1 |
| Fuzzy level | 7 | 5 | 10.9088 | 8.9158 | 7.1961 | 3.4860 | 2.6658 | 1.1844 | 1.0607 |
| | 2 | 4 | 11.4761 | 9.4012 | 7.6067 | 3.7063 | 2.7933 | 1.2320 | 1.0917 |
| | 7 | 2 | 10.3552 | 8.4405 | 6.7947 | 3.2708 | 2.5007 | 1.1378 | 1.0303 |
| | 3 | 5 | 11.3911 | 9.3281 | 7.5446 | 3.6736 | 2.8090 | 1.2248 | 1.0870 |
| | 2 | 7 | 11.6884 | 9.5846 | 7.7601 | 3.7885 | 2.8974 | 1.2498 | 1.1033 |
| | 5 | 4 | 10.9798 | 8.9754 | 7.2472 | 3.5134 | 2.6867 | 1.1903 | 1.0645 |
| | 2 | 6 | 11.6376 | 9.5399 | 7.7230 | 3.7687 | 2.8822 | 1.2455 | 1.1005 |
| | −5 | −5 | 11.1144 | 9.0907 | 7.3445 | 3.5656 | 2.7267 | 1.2016 | 1.0719 |
| | −4 | −6 | 11.3387 | 9.2831 | 7.5069 | 3.6527 | 2.7933 | 1.2204 | 1.0841 |
| Average value of $F_{O/(I+S)}$ | | | 11.2100 | 9.1733 | 7.4138 | 3.6028 | 2.7506 | 1.2096 | 1.0771 |

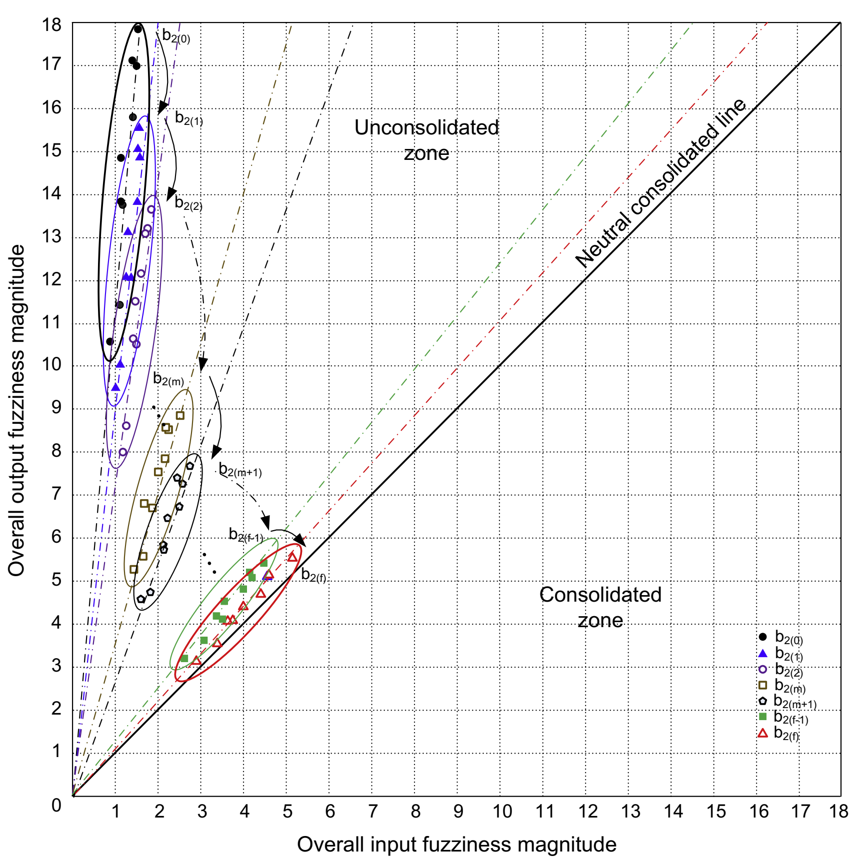


**Figure 8** Consolidity chart showing consolidity regions of change pathway of the drug concentration production problem for the ***conventional*** situation.

Please cite this article in press as: Gabr WI, A novel approach for system change pathway analysis using consolidity charts, Ain Shams Eng J (2015), http://dx.doi.org/10.1016/j.asej.2015.03.004

by gradually increasing the parameter $b_2$ (related to coefficient rate of flow of the drug from compartment #2 to outside). This pathway situation is in contrary to the gradual decrease of this parameter in the above system change pathway of the case study that could be caused by process malfunction. This yields using similar consolidity analysis of Table 2 the change pathway results summary:

| Event state $\mu$ | Parameter $b_2$ | Overall consolidity index $F_{O/(I+S)}$ | |
|---|---|---|---|
| 0 | 2.0 | 11.2100 | ***Deterioration*** ↓ |
| 1 | 2.1 | 12.2207 | |
| 2 | 2.2 | 13.0873 | |
| 3 | 2.3 | 14.0548 | |
| 4 | 2.5 | 16.2334 | |
| 5 | 2.7 | 20.9885 | |

The corresponding change pathway of the reverse situation of case study is plotted in Fig. 9. Such results show that there is a major deterioration of the overall consolidity index in the opposite direction. This is equivalent to the moving of consolidity regions in the chart from ***high*** to ***very high*** consolidity index zones ($F_{O/(I+S)} > 15.0$). Since the drug concentration problem is a ***man-made operation***, the above coefficient rate of flow of the drug from compartment #2 to outside could be adjusted to prevent its drift to the unwanted zone of high consolidity indices that would make the system parameters highly susceptible to changes under any noticeable events.

## 5. Implementation to prey–predator population problem

### 5.1. Model description

The problem of studying the populations between the prey and predator has assumed a prime importance due to its effect in ecology balance [9–11]. The problem can be extended to cover general species that compete, evolve and disperse simply for the purpose of seeking resources to sustain their struggle for their very existence. Depending on their specific settings of applications, they can take the forms of resource–consumer, plant–herbivore, parasite–host, tumor cells (virus)–immune system, susceptible–infectious interactions, etc. For the present prey–predator problem (such as rabbits versus fox problem), though the problem is mainly a pure natural one, man-made intervention could be possible through limiting the number of predators by killing, or increasing preys through hormone and other nutritious feeding. The target at the end is to keep the system balanced and avoiding one side to affect the reasonable growth of the other side.

The Prey–Predator population dynamics problem includes the effects of competing population, where one species may feed on another. This problem can be represented by two ordinary differential equations. Let $H(t)$ indicates the number of hares (prey) and $L(t)$ denotes the number of lynxes (predator).

The dynamics of the system can be expressed as [31]

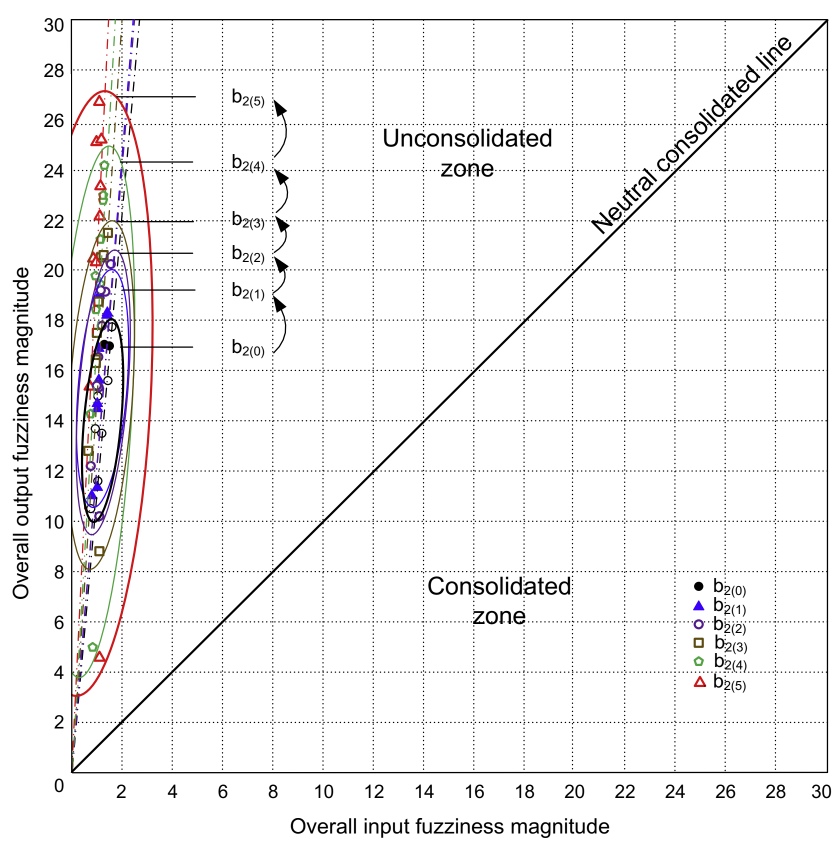


**Figure 9** Consolidity chart showing consolidity regions of the ***unconventional*** change pathway behavior of the drug concentration production problem.

**Table 3** Summary of consolidity pathway results of the prey–predator population problem.

| Aspect | Input parameters | | | | | Consolidity indices of $x_e$ | | | | | | |
|---|---|---|---|---|---|---|---|---|---|---|---|---|
| | $a$ | $b$ | $c$ | $d$ | $k$ | $r^{(0)}$ | $r^{(1)}$ | $r^{(2)}$ | $r^{(m)}$ | $r^{(m+1)}$ | $r^{(f-1)}$ | $r^{(f)}$ |
| Value | 3.2 | 0.6 | 50 | 0.56 | 125 | 0.5 | 1.0 | 1.5 | 3.0 | 3.5 | 4.5 | 5.0 |
| Fuzzy level | 5 | 8 | 4 | −2 | 2 | 4.9460 | 4.0965 | 3.5729 | 2.7703 | 2.6203 | 2.4021 | 2.3208 |
| | 5 | 5 | −1 | 3 | 3 | 4.9003 | 4.5106 | 4.2732 | 3.9199 | 3.8571 | 3.7696 | 3.7388 |
| | −1 | 2 | −2 | −4 | −1 | 5.2669 | 4.3073 | 3.7157 | 2.8075 | 2.6374 | 2.3896 | 2.3155 |
| | 2 | 1 | −2 | −4 | −2 | 5.0712 | 4.4931 | 4.1386 | 3.6020 | 3.5038 | 3.3636 | 3.3605 |
| | −4 | −3 | 4 | 1 | 2 | 5.4652 | 5.0335 | 4.9757 | 4.3793 | 4.3098 | 4.2130 | 4.3197 |
| | 1 | −1 | 2 | 6 | 1 | 6.0192 | 4.9060 | 4.2198 | 3.1659 | 2.9683 | 2.6803 | 2.5725 |
| | 5 | 5 | −3 | 2 | 4 | 5.9537 | 5.4450 | 5.1346 | 4.6708 | 4.5876 | 4.4713 | 4.4300 |
| | 6 | 7 | 2 | 2 | 2 | 5.3004 | 4.6818 | 4.3022 | 3.7275 | 3.6220 | 3.4712 | 3.4161 |
| | 4 | 5 | −2 | −2 | −3 | 5.6577 | 5.0428 | 4.6659 | 4.0987 | 3.9931 | 3.8451 | 3.7912 |
| Average value of $F_{o/(I+S)}$ | | | | | | 5.3979 | 4.7241 | 4.3332 | 3.6824 | 3.5666 | 3.4007 | 3.3628 |

$$\frac{dH}{dt} = rH\cdot\left(1-\frac{H}{k}\right) - \frac{aHL}{c+H}, \quad H \geqslant 0,$$
$$\frac{dL}{dt} = b\frac{aHL}{c+H} - dL, \quad L \geqslant 0 \tag{16}$$

In (16), the parameter $r$ represents the growth rate of the hares, $k$ designates the maximum population of the hares (in the absence of lynxes), $a$ represents the interaction term that describes how the hares are diminished as a function of the lynx population and $c$ controls the prey consumption rate for low hare population. In the second equation, $b$ denotes the growth coefficient of the lynxes and $d$ indicates the mortality of the lynxes.

There are three possible equilibrium points for this problem for $x_e = (L_e, H_e)$, namely [31].

$$x_e = \begin{bmatrix}0\\0\end{bmatrix},\ x_e = \begin{bmatrix}k\\0\end{bmatrix},\ \text{and } x_e = \begin{bmatrix}H_e^*\\L_e^*\end{bmatrix} \tag{17}$$

where $H_e^*$ and $L_e^*$ are given as

$$L_e^* = \frac{rH_e(c+H_e)}{aH_e}\cdot\left(1-\frac{H_e}{k}\right) = \frac{bcr\cdot(abk-cd-dk)}{(ab-d)^2k} \tag{18}$$

and

$$H_e^* = \frac{cd}{ab-d} \tag{19}$$

### *5.2. Consolidity chart for conventional system change pathway behavior*

In this case study, the change pathway of the prey–predator problem is left to the improving of climatic conditions that provide good plant feeding (vegetation density of the woody plants) that leads to corresponding increase of the growth rate of hares per unit time $r$ [10,11,27]. Stated otherwise, the event is rainfall that influences on the vegetation density and consequently would affect directly on the prey number. In fact, it was shown in a recent study, that such change in prey number relates linearly to the amount of rainfall [27].

As a demonstration of such effect on the consolidity chart during the problem conventional pathway change, the climate gradual increase was reflected to corresponding gradual change of parameter $r$ from a certain initial value of $r^{(0)} = 0.5$ to a final or end value of $r^{(f)} = 5.0$. The consolidity analysis will be implemented on the natural third equilibrium case of $x_e$ given in (17).

The results are shown in Table 3 and their consolidity chart during system change pathway is illustrated in Fig. 10, for seven chosen regions (three at the system beginning of its course of life, two at its intermediate life, and two at its ending life). The main finding of this Prey–Predator population problem is that the change of some systems parameters and control of the environment could improve the consolidity of the system. Such improvement has resulted in changing the overall consolidity index at the beginning of its course of life from $F_{o/(I+S)} = \mathbf{5.3979}$ **to** and ending value of $F_{o/(I+S)} = \mathbf{3.3628}$. Nevertheless, for this example additional experimentations are still needed to attain further improvement of such consolidity chart performance during change pathway in order to approach the neutral consolidated area.

### *5.3. Consolidity chart for unconventional system change behavior*

Let us now consider the ***unconventional*** change pathway behavior of the above prey–predator population problem by gradually decreasing the parameter $r$ (growth rate of the hares. This is in reverse of the change pathway conditions investigated in the above case study that could take place due to very poor continued environmental conditions. This provides using similar consolidity analysis of Table 3 the following pathway results summary:

| Event state $\mu$ | Parameter $r$ | Overall consolidity index $F_{O/(I+S)}$ | |
|---|---|---|---|
| 0 | 0.50 | 5.3979 | ***Deterioration ↓*** |
| 1 | 0.40 | 5.5864 | |
| 2 | 0.30 | 5.8018 | |
| 3 | 0.20 | 6.0500 | |
| 4 | 0.10 | 6.3354 | |
| 5 | 0.05 | 6.5028 | |

The corresponding change pathway of the reverse conditions of case study is sketched in Fig. 11. Such results illustrate slight deterioration of the overall consolidity index in the opposite direction. The movements of the consolidity regions are still within the lowest part of the **high** consolidity index

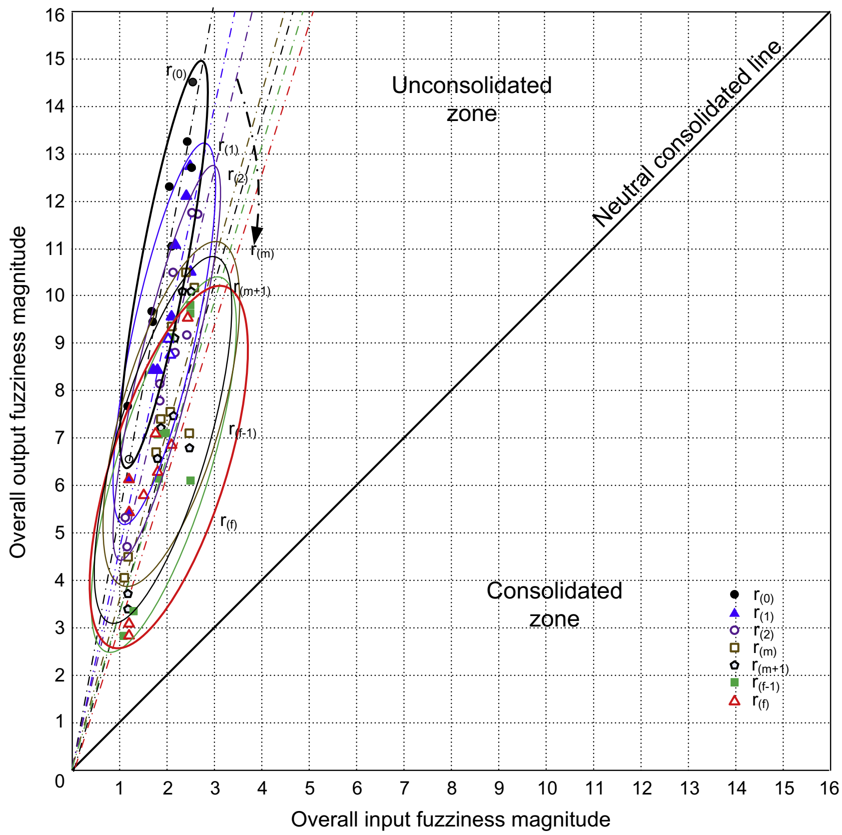


**Figure 10** Consolidity chart showing consolidity regions of change pathway of the prey–predator population problem for the ***conventional*** situation.

zone ($F_{O/(I+S)} > 5.0$). The shift to such level of high consolidity index is still manageable in real life revealing the relative environmental balance of the prey–predator process.

## 6. Implementation to spread of infectious diseases problem

### 6.1. Model description

The investigation of spread of infectious disease is also one of the important problems affecting population health. Overcrowded cities or densely populated areas of cities can potentially serve as breeding grounds for infectious agents, which may facilitate their evolution, particularly in the case of viruses and bacteria. Usually, the problem concentrates on invoking ways to reduce the rate of spread of certain infectious disease by various means such as **vaccination** and conducting effective ***hygienic awareness programs*** for enhancing the habits of population under infection risk [32].

In this case study, we have a total population of $N$ people and a certain contagious disease infecting this population. Let us call this disease $D$. This population is split up at any time $t$ into three groups as follows:

(i) $x(t)$ = those uninfected with $D$ but may become infected,
(ii) $y(t)$ = those who are presently infected with $D$ and can spread the disease, and
(iii) $z(t)$ = those who had the disease $D$ and are dead, recovered and immune, or isolated and cannot spread the infection. We always have $N = x(t) + y(t) + z(t)$ for $t \geqslant 0$.

Our first assumption is that the rate of transfer from $x$ into $y$ is directly proportional to $x{\cdot}y$. Or, $\dot{x} = -kx \cdot y$ for certain positive constant $k$, to be designated as the infection rate. This parameter needs to be estimated. The rate of transfer into $y$ comes from $x$ but the rate of transfer out of $y$ goes to $z$. The rate out of $y$ is assumed to be proportional to $y$. The differential equation is $\dot{y} = k \cdot x \cdot y - c \cdot y$ for some positive constant (the removal rate) $c$. This constant will also need to be estimated. If we differentiate $N = x + y + z$ and solve for $dz/dt$ we obtain $dz/dt = c{\cdot}y$. But we do not need this third differential equation because we may always find $z$ from $z = N - x - y$. Therefore, the system of nonlinear differential equations to solve is expressed as [10]

$$\dot{x} = -kx \cdot y \tag{20}$$

$$\dot{y} = k \cdot x \cdot y - c \cdot y \tag{21}$$

and

$$z = N - x - y \tag{22}$$

such as $x(t)$ represents those uninfected with disease but may become infected, $y(t)$ indicates those who are presently infected with the disease, $k$ represents the infection rate, and $c$ is the removal rate. The two parameters $k$ and $c$ are modeled as fuzzy

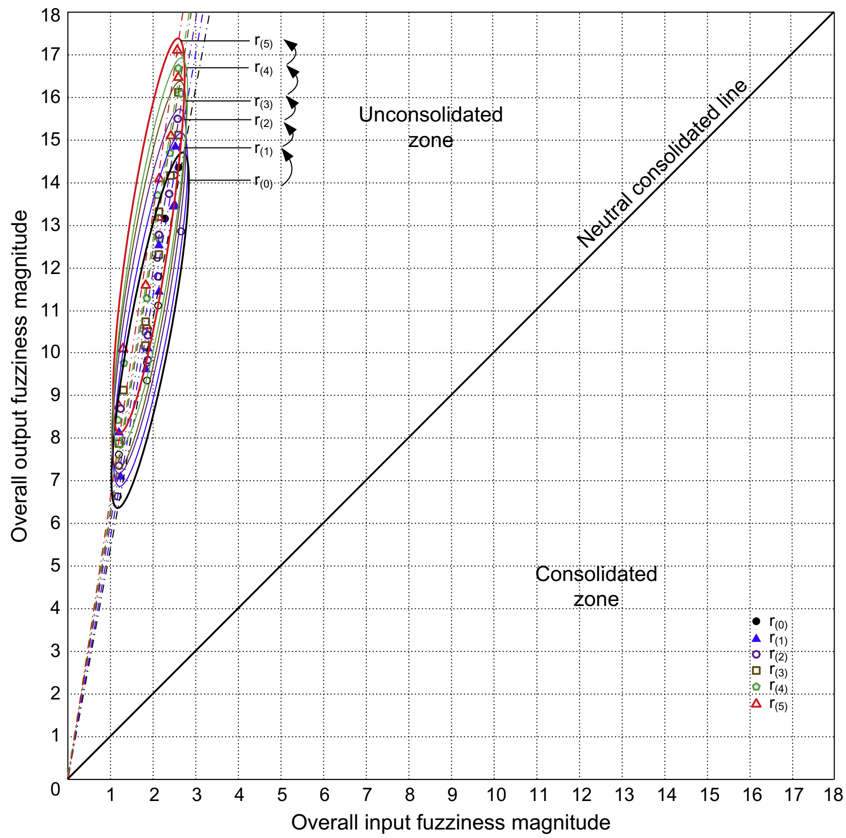


**Figure 11** Consolidity chart showing consolidity regions of the ***unconventional*** change pathway of the prey–predator population problem.

**Table 4** Summary of consolidity pathway results of the spread of infectious disease problem.

| Aspect | Input parameters | | | Consolidity indices of the linearized model | | | | | | |
|---|---|---|---|---|---|---|---|---|---|---|
| | $c$ | $x_0$ | $y_0$ | $k^{(0)}$ | $k^{(1)}$ | $k^{(2)}$ | $k^{(m)}$ | $k^{(m+1)}$ | $k^{(f-1)}$ | $k^{(f)}$ |
| Value | 0.9 | 950 | 50 | 0.1 | 0.09 | 0.08 | 0.04 | 0.03 | 0.005 | 0.001 |
| Fuzzy level | 6 | 6 | 2 | 7.9212 | 7.2328 | 6.5437 | 3.7869 | 3.0975 | 1.3690 | 1.0652 |
| | 5 | 4 | 3 | 9.8558 | 8.9708 | 8.0860 | 4.5463 | 3.6613 | 1.4420 | 1.0524 |
| | 7 | 5 | 3 | 9.1707 | 8.3552 | 7.5396 | 4.2773 | 3.4616 | 1.4157 | 1.0548 |
| | 6 | 1 | 1 | 7.1227 | 6.5144 | 5.9061 | 3.4731 | 2.8648 | 1.3404 | 1.0776 |
| | 5 | 7 | 1 | 7.0084 | 6.4116 | 5.8152 | 3.4281 | 2.8312 | 1.3349 | 1.0729 |
| | 5 | 2 | 1 | 8.6835 | 7.9165 | 7.1500 | 4.0834 | 3.3166 | 1.3918 | 1.0436 |
| | 1 | 1 | 1 | 10.9145 | 9.9220 | 8.9294 | 4.9584 | 3.9656 | 1.4769 | 1.0429 |
| | 1 | 2 | 1 | 8.6846 | 7.9177 | 7.1512 | 4.0849 | 3.3182 | 1.3966 | 1.0634 |
| | 5 | 3 | 2 | 9.4678 | 8.6218 | 7.7762 | 4.3932 | 3.5471 | 1.4254 | 1.0495 |
| Average value of $F_{O/(I+S)}$ | | | | 8.7588 | 7.9848 | 7.2108 | 4.1146 | 3.3404 | 1.3992 | 1.0580 |

variables and depend on the type of disease, the season (winter or summer), whether or not the population has been vaccinated against $D$, etc. Experts in infectious diseases are usually familiar of the way for estimating $k$ and $c$.

### *6.2. Consolidity chart for conventional system change pathway behavior*

The parameter $k$ which represents the rate of transfer of the disease is closely influenced by combined vaccination and enhancing population hygiene practice. Enhancing such practice through awareness and school education will lead to reducing the infection rate of the spread of infectious diseases [10,32]. In fact, it was shown in a recent study that such reduction in infectious disease spread relates exponentially to such awareness efforts [27]. To demonstrate the influence of vaccination and improving hygiene practice on the conventional pathway change cycle of any infectious disease, we will start with unvaccinated population with very bad hygienic practice with a starting value of $k^{(0)} = 0.1$ and gradually increasing their vaccination and improving population hygienic practice leading to a combined effective ending level of $k^{(f)} = 0.001$.

Please cite this article in press as: Gabr WI, A novel approach for system change pathway analysis using consolidity charts, Ain Shams Eng J (2015), http://dx.doi.org/10.1016/j.asej.2015.03.004

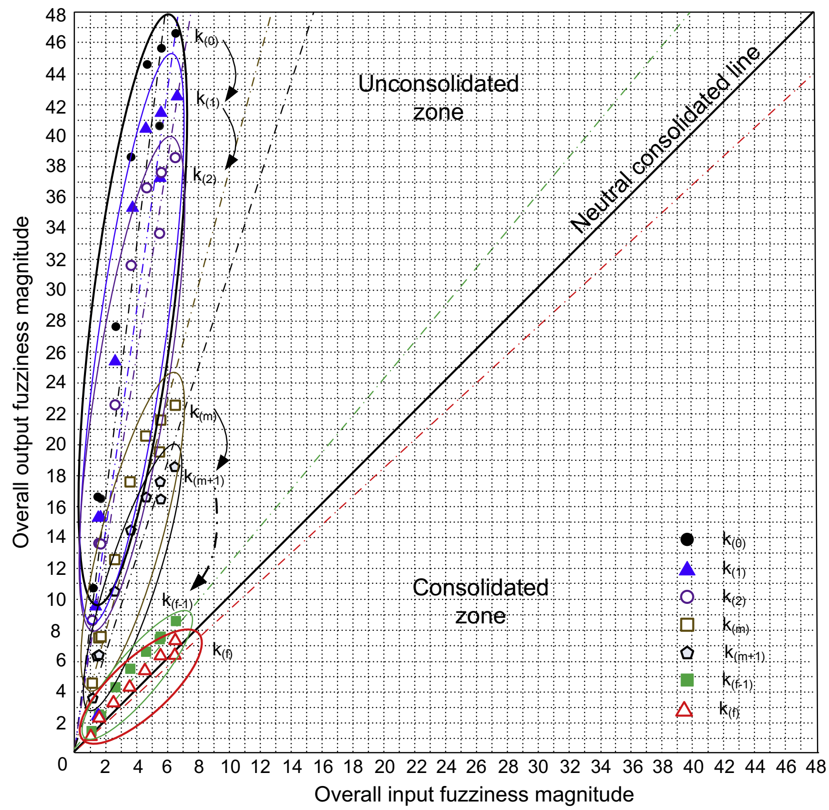


**Figure 12** Consolidity chart showing consolidity regions of change pathway of the spread of infectious disease problem for the ***conventional*** situation.

The system is firstly linearized around its operating points and its consolidity analysis was then carried out for the changing values of the infection rate $k^{(\mu)}$ corresponding to each event step $\mu$. The results are shown in Table 4, with the consolidity chart of the problem is plotted in Fig. 12. In the figure, the consolidity chart is sketched using 7 different states, three at the beginning of conducting the vaccination and hygienic awareness campaign, two at intermediate state, and the last two states are the ending ones. The chart reveals the considerable improvement in consolidity from very high overall value ***unconsolidated state*** of $F_{O/(I+S)} = 8.7588$ at the start of the vaccination and awareness campaign and ending to almost nearly ***neutral consolidated state*** value of $F_{O/(I+S)} = 1.0580$ at the end of the combined vaccination and awareness campaigns.

### *6.3. Consolidity chart for unconventional system change behavior*

We will consider now the ***unconventional*** change pathway behavior case of the spread of infectious diseases problem by reversing the changes in the parameter $k$ (infection rate or rate of transfer of the disease). This is in contrary to the change pathway analysis of the case study that may occur due to continual poor ***vaccination*** and conducting ineffective ***hygienic awareness programs***. This gives using similar consolidity analysis of Table 4 the following pathway results summary:

| Event state $\mu$ | Parameter $k$ | Overall consolidity index $F_{O/(I+S)}$ | |
|---|---|---|---|
| 0 | 0.10 | 8.7588 | ***Deterioration*** ↓ |
| 1 | 0.12 | 10.3069 | |
| 2 | 0.14 | 11.8550 | |
| 3 | 0.16 | 13.4034 | |
| 4 | 0.18 | 14.9513 | |
| 5 | 0.21 | 17.5825 | |

The corresponding change pathway of the reverse conditions of case study is shown in Fig. 13. Such results illustrate rapid deterioration of the overall consolidity index in the reverse direction. The movements of the consolidity regions are very fast moving from the ***high*** to the ***very high*** consolidity index zone ($F_{O/(I+S)} > 15.0$). Moreover, these results reveal that once the value of parameter $k$ (rate of transfer of the disease) increases corresponding jump of overall consolidity index takes place. Such results lucidly describe the mechanism of failing to control the spread of infectious diseases. As the system consolidity index grows to higher levels, the system parameters become more susceptible to changes upon the effect of any ***external*** or ***internal*** influences leading to consecutive higher rates of the spread of diseases.

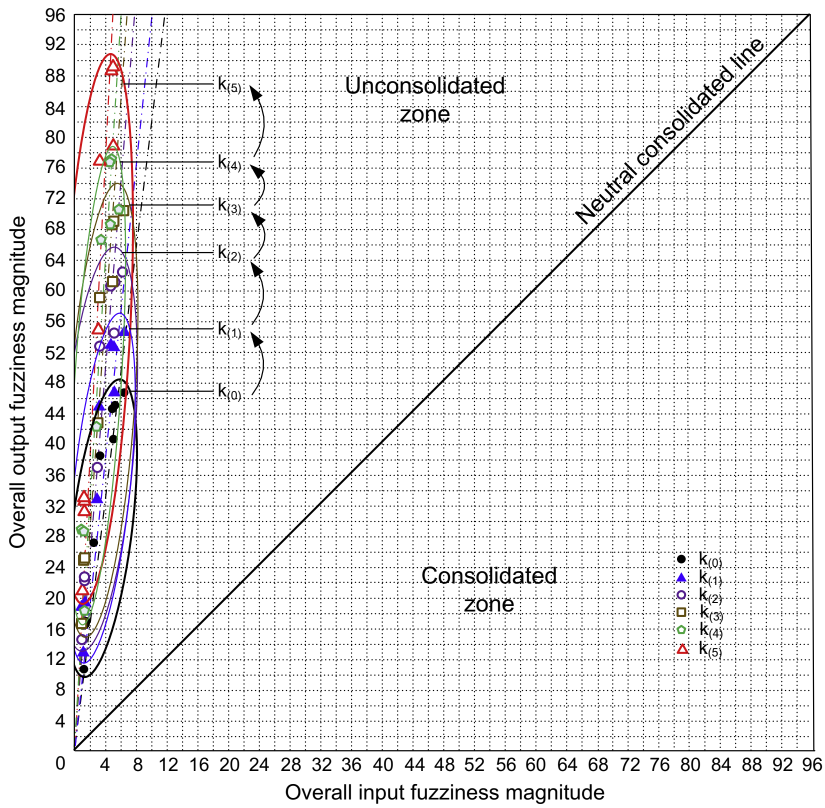


**Figure 13** Consolidity chart showing consolidity regions of the ***unconventional*** change pathway behavior of the spread of infectious disease problem.

**Table 5** Summary of consolidity pathway results of the HIV/AIDS Epidemic problem.

| Aspect | Input parameters | | | | | Consolidity indices of controllability matrix $\|M\|$ | | | | | | |
|---|---|---|---|---|---|---|---|---|---|---|---|---|
| | $k_2$ | $k_3$ | $k_4$ | $k_5$ | $b$ | $a^{(0)}$ | $a^{(1)}$ | $a^{(2)}$ | $a^{(m)}$ | $a^{(m+1)}$ | $a^{(f-1)}$ | $a^{(f)}$ |
| Value | 0.025 | 0.7 | 0.2 | 1 | 0.3 | 2.0 | 1.8 | 1.6 | 0.5 | 0.4 | 0.2 | 0.1 |
| Fuzzy levels | 3 | 5 | 2 | 1 | 3 | 12.8477 | 12.0752 | 12.0752 | 4.6637 | 3.6609 | 1.6208 | 0.8614 |
| | 2 | 6 | 3 | 2 | 7 | 12.0995 | 11.3732 | 11.3732 | 4.4338 | 3.4990 | 1.5999 | 0.8938 |
| | 4 | 3 | 4 | 2 | 4 | 14.1986 | 13.3536 | 13.3536 | 5.2916 | 4.2026 | 1.9785 | 1.1410 |
| | 3 | 1 | 7 | 3 | 3 | 12.3317 | 11.6596 | 11.6596 | 6.4909 | 5.1766 | 1.6715 | 0.9358 |
| | 2 | 4 | 5 | 2 | 3 | 12.5707 | 11.8199 | 11.8199 | 5.6536 | 4.4713 | 1.6349 | 0.8803 |
| | 6 | 3 | 4 | 1 | 6 | 13.9145 | 13.4121 | 13.4121 | 6.4069 | 5.1959 | 1.8839 | 1.0424 |
| | −2 | −3 | −2 | −1 | −2 | 12.3605 | 11.7164 | 11.7164 | 4.8984 | 3.8506 | 1.8089 | 1.1701 |
| | 6 | 4 | 3 | 1 | 7 | 15.6125 | 14.6752 | 14.6752 | 5.5217 | 4.4589 | 2.0478 | 1.1339 |
| | 3 | 6 | 4 | 2 | 6 | 12.1273 | 11.4053 | 11.4053 | 4.8876 | 3.8656 | 1.6491 | 0.9256 |
| Average value of $F_{O/(I+S)}$ | | | | | | 13.1181 | 12.3878 | 11.8949 | 5.3609 | 4.2646 | 1.7662 | 0.9983 |

## 7. Implementation to HIV/AIDS Epidemic problem

### 7.1. Model description

The problem of ***HIV/AIDS Epidemic*** has attracted the interest of many researchers in the last two decades due to its importance. This term HIV/AIDS abbreviates Human ***immunodeficiency virus infection*** and ***acquired immune deficiency syndrome*** which is a disease of the human immune system caused by infection with human immunodeficiency virus (HIV). There are many causes of HIV/AIDS, but our investigation in this case study will concentrate on its spread due to males' homosexual behavior [33–35].

For this case study, the consolidity analysis of the problem of the HIV/AIDS Epidemic is considered for a specific geographical region with high homosexual males' population. There is a constant immigration rate $k_1$ of susceptible males into the population of size $N(t)$. In this model the size of the population $N(t)$ can change in time, where the population size was fixed.

Please cite this article in press as: Gabr WI, A novel approach for system change pathway analysis using consolidity charts, Ain Shams Eng J (2015), http://dx.doi.org/10.1016/j.asej.2015.03.004

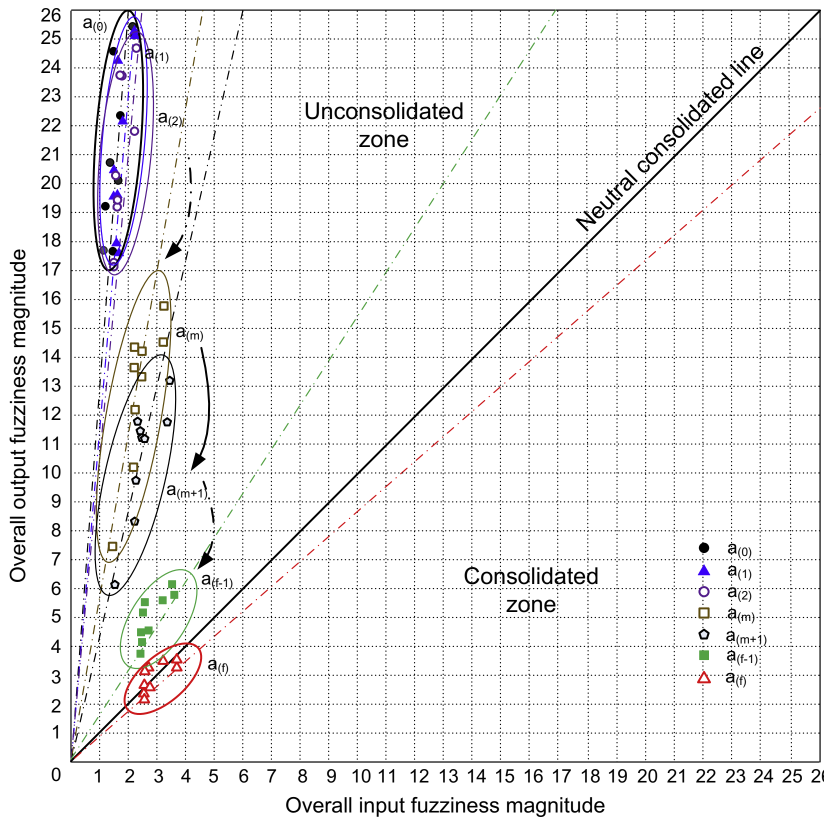


**Figure 14** Consolidity chart showing consolidity regions of change pathway of the HIV/AIDS Epidemic problem for the ***conventional*** situation.

The model describing the HIV/AIDS Epidemic system can be expressed as [10]:

$$\dot{X} = k_1 - k_2X - a \cdot k_3X \quad (23)$$

$$\dot{Y} = ak_3X - (k_4 + k_2) \cdot Y \quad (24)$$

$$\dot{Z} = (1 - b) \cdot k_4Y - k_2Z \quad (25)$$

$$\dot{A} = bk_4Y - (k_2 + k_5) \cdot A \quad (26)$$

and

$$N(t) = X(t) + Y(t) + Z(t) + A(t) \quad (27)$$

such that $N(t)$ is the population size, $X(t)$ denotes the number of susceptible males in the population, $Y(t)$ designates the number of males infected with HIV virus, $Z(t)$ represents the number of males infected with virus but is non-infections, and $A(t)$ is the number of men with AIDS. The parameters $k_2$, $k_3$, $k_4$, $k_5$ and $b$ are modeled as fuzzy parameters, $k_1$ is a constant and parameter $a$ representing Average number of different sexual partners per year will be assumed to be the influenced factor in the problem change pathway. Now, Eqs. (23)–(27) can be rewritten in the state space, to enable the advanced control theory concepts such as *stability* and *controllability* can be applied, as follows [36–38]:

$$\begin{bmatrix} \dot{X} \\ \dot{Y} \\ \dot{Z} \\ \dot{A} \end{bmatrix} = \begin{bmatrix} -k_2 - a \cdot k_3 & 0 & 0 & 0 \\ a \cdot k_3 & -k_2 - k_4 & 0 & 0 \\ 0 & (1-b) \cdot k_4 & -k_2 & 0 \\ 0 & b \cdot k_4 & 0 & -k_2 - k_5 \end{bmatrix} \cdot \begin{bmatrix} X \\ Y \\ Z \\ A \end{bmatrix} + \begin{bmatrix} k_1 \\ 0 \\ 0 \\ 0 \end{bmatrix} \quad (28)$$

For $k_1 = 13\frac{1}{3}$ (Thousands inhabitants), and for various state scenario of $a$, the consolidity analysis was carried out by investigating the determinant of the controllability matrix of this system denoted by $|M|$ where the controllability measures the degree that the system can be controlled, such that a control exists that will transfer the system from any initial state $x(0)$ to some final state $x(t)$ in a finite time interval.

It follows from (23) and (24) and the state space approach that the open transfer functions of $X(s)$ and $Y(s)$ can be expressed as:

$$X(s) = \frac{k_1}{(s + k_2 + ak_3)} \quad (29)$$

and

$$Y(s) = \frac{ak_1k_3}{(s + k_2 + ak_3) \cdot (s + k_4 + k_2)} \quad (30)$$

which represent stable transfer function for all range of $a > 0$, though their corresponding systems are unconsolidated (or highly) unconsolidated.

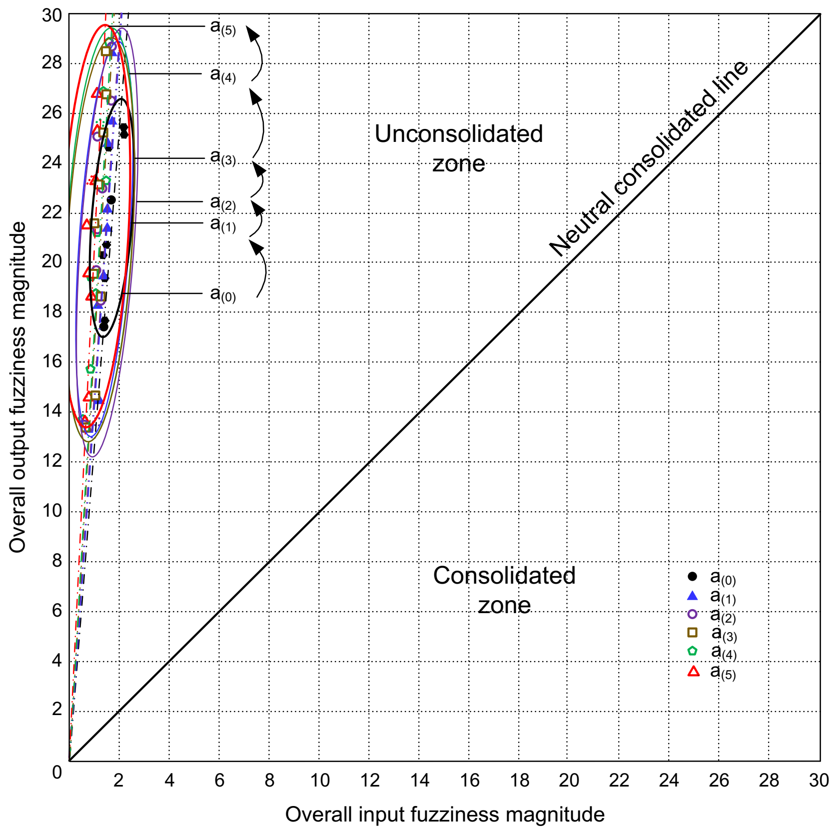


**Figure 15** Consolidity chart showing consolidity regions of the ***unconventional*** change pathway behavior of the HIV/AIDS Epidemic problem.

In fact, it appears from (29) that as the parameter $a$ decreases, the system gets less stable while the consolidity index $F_{O/(I+S)}$ gets smaller indicating higher consolidity. This lucidly reveals the opposite effect of changes of parameters on consolidity versus stability.

### 7.2. Consolidity chart for conventional system change pathway behavior

For this case study, the parameter $a$ representing average number of different sexual partners per year is considered the primary factor influencing the problem change pathway. The effectiveness of awareness and educational campaigns in reducing the risk of sexual transmission of the human immunodeficiency virus (HIV) and certain other sexually transmitted infections (STIs) has been well established [35]. In fact, it was reported in a recent study, such reduction in sexual transmission risk relates exponentially to such awareness efforts [27].

Following this issue, the change pathway of the HIV/AIDS problem will be handled for the conventional situation by making influence of such awareness campaigns in gradually reducing the parameter $a$ from an initial value of $a^{(0)} = 2.0$ gradually to a final ending value of $a^{(f)} = 0.1$. The corresponding results are shown in Table 5, with the consolidity chart of the problem is plotted in Fig. 14. In this figure, the consolidity chart is demonstrated by five different event states, three at the beginning of awareness campaigns, two at intermediate stage, and the last two are at the ending stage of awareness campaigns. This has led in shifting the situation from completely ***unconsolidated state*** of $F_{O/(I+S)} = 12.1273$ to a final ***consolidated state*** of $F_{O/(I+S)} = 0.9256$ at the end of awareness campaigns.

### 7.3. Consolidity chart for unconventional system change behavior

We will investigate now the ***unconventional*** change pathway behavior situation for the HIV/AIDS Epidemic problem when the parameter $a$ (average number of different sexual partners per year) changes in the opposite direction. This is in contrary of the solved system change pathway of the case study that may take place due to poor influence of the HIV/AIDS awareness campaigns. This gives using similar consolidity analysis of Table 5 the following pathway results:

| Event state $\mu$ | Parameter $a$ | Overall consolidity index $F_{O/(I+S)}$ | |
|---|---|---|---|
| 0 | 2.0 | 13.1181 | ***Deterioration*** ↓ |
| 1 | 2.3 | 14.5440 | |
| 2 | 2.7 | 15.9882 | |
| 3 | 3.0 | 17.1571 | |
| 4 | 3.5 | 18.4753 | |
| 5 | 4.0 | 20.9321 | |

The corresponding change pathway of the reverse situations of case study is illustrated in Fig. 15. Such results reveal continuous deterioration of the overall consolidity index in the

Please cite this article in press as: Gabr WI, A novel approach for system change pathway analysis using consolidity charts, Ain Shams Eng J (2015), http://dx.doi.org/10.1016/j.asej.2015.03.004

reverse direction. The movements of the consolidity regions are fast moving from the ***high*** to the ***very high*** consolidity index zone ($F_{O/(I+S)} > 15.0$). The above results demonstrate that the parameter $a$ of the average number of different sexual partners per year is very crucial for the susceptibility of the HIV/AIDS Epidemic problem to withstand changes in its spreading action. The increase of such parameter beyond certain level could definitely lead to corresponding high rate of the sweeping of such infection.

Similar consolidity pathway treatment can be applied to other potential problems such as: i) three species competitions model, ii) symbiosis model, iii) biological circuitry model, iv) insulin-glucose dynamic (drug administration) model, v) atomic force microscopy model, vi) coupled spring mass system model, and vii) national economy model [10,31].

## 8. Other applications and works

The application of consolidity charts and consolidity pathway is an effective tool and is open now for intense future research for many real life disciplines problems and fields. Examples of such promising fields can be foreseen as follows: (i) evolutionary sciences, engineering, materials sciences, nanotechnology, astronomy, informatics, and behavioral sciences; (ii) biology, genetics, genomics, medicine, health, psychiatry, dentistry, veterinary medicine, pharmacology, genetics, and bioinformatics; (iii) geology, archeology, physical anthropology, life sciences, ecology, environmental sciences, botany, agronomy, hydrology, oceans sciences, etc., and (iv) social sciences, psychology, philosophy, geography, political sciences, education, mass communications, performing arts, visual arts, and athletics.

Other works could be directed toward the implementation of the consolidity chart approach for analyzing multi-systems with mutual changes and interactions, and also for handling the wide-range interactions between everywhere real life systems during their change pathways. Another point of important research is to carry out the field investigations of the consolidity region concept through real life measurements and experimentations, and also testing of the approach through building emulators-based that can perform combined hardware/software co-simulation of the original system. The study could also include developing appropriate tools for modeling of the predictive future system behavior.

## 9. Conclusions

This paper has addressed one of the real life important problems which is the analysis of systems change pathway. This problem has attracted the attention of a wide spectrum of experts and researchers as it is closely linked to all living beings and materials course of life. All systems either man-made or natural are subject to deterioration, degrading, aging, etc. The introduction of the new approach of consolidity chart for studying such problem represents an addition for the investigation of such problem. Consolidity index by itself is the system internal metric responsible on scaling system change of parameters when the system is affected by internal or external influences or events "***on and above***" its normal situations or set points.

The study of the consolidity chart during the system course of life has led to the appearance of consolidity regions and the new ***consolidity pathway trajectory***. Such trajectory gives an in-depth view of how the system is changing during its course of life under influences of various types and directions. These pathway changes are considered for both ***conventional*** and ***unconventional*** system change pathway behaviors.

Due to the complexity of the problem, the investigation was limited to the effect of changing one key system parameter that changes with the life progress of the system. Such parameter could change due to natural causes or due to external human intervention (or due to both factors). Several illustrative examples were presented to explain such ***consolidity pathway trajectory*** concept using only one parameter changing for each case study during its course of life. The regions comparison with consolidity chart could then be based on type of consolidity region shape such as elliptical or circular, slope or angle in degrees of the centerline of the geometric, the centroid of the geometric shape, area of the geometric shape, length of major and minor diagonals of the shape, and the diversity ratio of consolidity points for each region.

Four case studies from life sciences, biology, and medicine were solved to demonstrate how their life cycle pathways change in real life situation for both conventional and nonconventional situations. The results showed how the consolidity regions change toward increases or decreases of the overall consolidity. Shapes and sizes of these regions differ from one case to another and from one state to the next ones. Such sizes of consolidity regions have marked the boundary of all system interactive behavior resulting from all exhaustive ***internal*** and ***external*** influences.

Real life problems are not in fact of such **simplicity** as presented in the given case study. System is influenced during its change pathway with many influencing (rather than one) parameters. Such influences will cause the system to go ***hence and forth*** (up and down) but resulting effects always prevail to shape at the end the way, the consolidity pathway trajectory should go in a certain neat or geometric or zigzagging form to its intermediate then to the system ending or final state. In this regard, each system will have its specific trajectory depending on how it affected by consecutive events of different types, strength and direction.

## Acknowledgments

The author is grateful to Nord Professor of Engineering and Chair **Dr. Kenneth A. Loparo** and Research Associate Professor **Dr. Richard M. Kolacinski**, Dept. of Electrical Engineering and Computer Science, Case Western Reserve University (Cleveland, Ohio, USA) for their sincere support.

## References

[1] Dorrah HT. Supplement to "Consolidity: Moving opposite to built-as-usual systems practice". Elsevier Ain Shams Eng J – ASEJ 2013;4(4):783–803. http://dx.doi.org/10.1016/j.asej.2013.02.009.

[2] Dorrah HT. Consolidity: stack-based systems change pathway theory elaborated. Elsevier Ain Shams Eng J – ASEJ 2014;5(2):449–73. http://dx.doi.org/10.1016/j.asej.2013.12.002.

[3] Dorrah HT. Toward a new "Fractals-general science". Elsevier Alexandria Eng J – AEJ 2014;53(3):505–12. http://dx.doi.org/10.1016/j.aej.2014.07.003 [Short Communication].

Please cite this article in press as: Gabr WI, A novel approach for system change pathway analysis using consolidity charts, Ain Shams Eng J (2015), http://dx.doi.org/10.1016/j.asej.2015.03.004

[4] Lemaitre J, Desmorat R. Engineering damage mechanics: ductile, creep, fatigue and brittle failure. New York: Springer-Verlag, Berlin and Heidelberg Co.; 2005.
[5] Anastasios P, Vassilopoulos P, editors. Fatigue life prediction of composites and composite structures. Cambridge UK: Woodhead Publishing Series in Composites Science and Engineering No. 30, CRC Press; 2010.
[6] Bathias C, Pineau A. Fatigue of materials and structures: application to design. New York: John Wiley & Sons Inc.; 2013.
[7] Neri E, Caramella D, Bartolozz C, editors. Image processing in radiology – current applications. New York: Springer-Verlag, Berlin Heidelberg; 2008.
[8] Kriete A, Bosl WJ, Booker G. Rule-based cell systems model of aging using feedback loop motifs mediated by stress response. PLOS Comput Biol 2010:1–13 [journal.pcbi.1000820].
[9] Hwang ES, Yoon G, Kang HT. A comparative analysis of the cell biology of senescence and aging. Cell Mol Life Sci 2009;66:2503–24.
[10] Buckley JJ, Jowers LJ. Simulating continuous fuzzy systems. Berlin: Springer; 2006.
[11] Balme G, Hunter L, Slotow R. Feeding habitat selection by hunting leopards Panthera pardus in a woodland savanna: prey catchability versus abundance. Anim Behav – ANBEHAV 2007;74:589–98.
[12] Zenil H, editor. A computable universe – understanding and exploring nature and computation. New Jersey, USA: World Scientific Publishing; 2012.
[13] Takeuchi Y, Iwasa Y, Sato K, editors. Mathematics for life science and medicine. New York: Springer-Verlag, Berlin Heidelberg; 2007.
[14] Albeverio S, Jentsch V, Kantz H, editors. Extreme events in nature and society. New York: Springer Science + Business Media Inc.; 2005.
[15] Kreith F, Goswami DY, editors. The CRC handbook of mechanical engineering. Danvers, MA, USA: CRC Press; 2005.
[16] De Paoli F, Tisato F. On the complementary nature of event-driven and time-driven models. Control Eng Pract 1996;4(6):847–54.
[17] Cassandras CG, Lafortune S. Introduction to discrete event systems, 2nd ed. New York: Springer Science + Business; 2008.
[18] Doney A, Garcia AL, Alder BJ. Stochastic event-driven molecular dynamics. J Comput Phys 2008;227:2644–65.
[19] Miller S, Luding S. Event-driven molecular dynamics in parallel. J Comput Phys 2003;193:306–16.
[20] Zimmermann A. Stochastic discrete event systems – modeling, evaluation, applications. Berlin: Springer Science + Business Media Inc.; 2008.
[21] Cezon M, Wolfsthal Y, editors. A new biology: a modern perspective on the challenge of closing the gap between the islands of knowledge. Service wave 2010 workshops, LNCS 6569. Berlin Heidelberg: Springer-Verlag; 2011. p. 188–95.
[22] Dorrah HT, Gabr WI. Foundations of new systems' consolidity theory using arithmetic fuzzy logic-based representation in fully fuzzy environment. In: Proceedings of 6th annual IEEE conference on automation science and engineering (IEEE CASE), Toronto, Ontario, Canada, August 21–24; 2010. p. 624–31 [Paper No. MoC2.1.].
[23] Dorrah HT, Gabr WI. Development of new consolidity theory for systems' analysis and design in fully fuzzy environment. Int J Expert Syst Appl – ESWA 2012;39(1):1191–9. http://dx.doi.org/10.1016/j.eswa.2011.07.125.
[24] Dorrah HT. Consolidity: mystery of inner property of systems uncovered. Elsevier J Adv Res – JARE 2012;3(4):345–58. http://dx.doi.org/10.1016/j.jare.2011.11.002.
[25] Dorrah HT. Consolidity: moving opposite to built-as-usual systems practices. Elsevier Ain Shams Eng J – ASEJ 2013;4(2):221–39. http://dx.doi.org/10.1016/j.asej.2012.07.004.
[26] Gabr WI. Consolidity analysis of fuzzy functions, matrices, probability and statistics. Elsevier Ain Shams Eng J 2014;6(1):181–97. http://dx.doi.org/10.1016/j.asej.2014.09.014.
[27] Ginidi RRG. Development of new system paradigm based on "time driven-event driven-parameters changes" with applications. Ph.D. thesis. Dept. Electrical Power and Machines, Faculty of Engineering, Cairo University, Giza, Egypt; 2015.
[28] Gabr WI. Arithmetic fuzzy logic-based representation approach versus conventional fuzzy theory for modeling and analysis in fully fuzzy environment. In: Proceedings of IEEE international conference on information and automation (ICIA 2010), Harbin, Heilongjiang, China, June 20–23; 2010 [Paper No. 1031751], p. 637–43.
[29] Gabr WI. Analogy between arithmetic fuzzy logic-based representation approach and conventional fuzzy theory with applications to operations research. J Al Azhar Univ Eng Sector (JAUES) 2015; 10(1), Paper No. 35, ISSN 1110-6409.
[30] Bailey JM, Haddad WM. Drug dosing control in clinical pharmacology. IEEE Control Syst Mag 2005;April:33–51.
[31] Astrom KJ, Murray RM. Feedback systems – an introduction for scientists and engineers. Princeton and Oxford: Princeton University Press; 2008.
[32] Miko BA, Cohen B, Conway L, Gilman A, Seward Jr SL, Larson E. Determinants of personal and household hygiene among college students in New York City, 2011. Am J Infect Control J – AJIC 2012:940–5.
[33] Parham P. The immune system, 3rd ed. New York: Garland Science, Taylors & Francis Group; 2009.
[34] Dasgupta D. Advances in artificial immune systems. IEEE Comput Intell Mag 2006;November:40–9.
[35] Bessingera R, Katendeb C, Guptac N. Multi-media campaign exposure effects on knowledge for STI and HIV/AIDS prevention in Uganda. Eval Program Plan J – EVALPROGPLAN 2004;27:397–407.
[36] Burns RS. Advanced control engineering. Oxford, UK: Butterworth Heinemann, Reed Elsevier Group; 2001.
[37] Ogata K. Modern control engineering. Upper Saddle River, New Jersey: Pearson Education International Prentice Hall; 2010.
[38] Gabr WI. A new approach for automatic control modeling, analysis and design in fully fuzzy environment. Elsevier Ain Shams Eng J – ASEJ 2015. http://dx.doi.org/10.1016/j.asej.2015.01.010, in press.

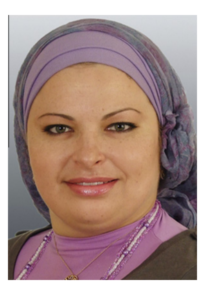

**Dr. Walaa Ibrahim Gabr** received her B.Sc. in Electrical Engineering from Benha University (Shoubra Faculty), Egypt in year 2000, and the M.Sc. and Ph.D. Degrees in Automatic Control from Cairo University, Egypt, in 2006 and 2008 respectively. She is currently an Assistant Professor of Electrical Engineering, Benha Engineering Faculty, Benha University, Egypt. Since March 2015, she is also a Visiting Assistant Professor with the Dept. of Electrical Engineering and Computer Science, Case Western Reserve University (Cleveland, Ohio, USA). From 2009 till 2010, she worked as Research and Development Senior Consultant with SDA Engineering Canada Inc. (Toronto, Ontario) in the area of intelligent systems and their applications. In year 2010, she developed jointly with Dr. Hassen Taher Dorrah (Cairo University) the new concept of "***Consolidity Theory***" as one of the inner properties of both *natural* and *man-made* systems and shared with him most of its following research works and advancements. Her main interests are system engineering, automatic control, intelligent systems, fuzzy systems, optimization techniques, probability and statistics, operations research, and smart power grids.